Neurochemical Research
https://doi.org/10.1007/s11064-022-03623-y

ORIGINAL PAPER

Rho–Rho-Kinase Regulates Ras-ERK Signaling Through SynGAP1 for Dendritic Spine Morphology

Mengya Wu[1] · Yasuhiro Funahashi[2] · Tetsuya Takano[3,4] · Emran Hossen[2] · Rijwan Uddin Ahammad[2] · Daisuke Tsuboi[2] · Mutsuki Amano[1] · Kiyofumi Yamada[5] · Kozo Kaibuchi[1,2]

Received: 28 November 2021 / Revised: 14 April 2022 / Accepted: 18 April 2022

Abstract

The structural plasticity of dendritic spines plays a critical role in NMDA-induced long-term potentiation (LTP) in the brain. The small GTPases RhoA and Ras are considered key regulators of spine morphology and enlargement. However, the regulatory interaction between RhoA and Ras underlying NMDA-induced spine enlargement is largely unknown. In this study, we found that Rho-kinase/ROCK, an effector of RhoA, phosphorylated SynGAP1 (a synaptic Ras-GTPase activating protein) at Ser842 and increased its interaction with 14-3-3ζ, thereby activating Ras-ERK signaling in a reconstitution system in HeLa cells. We also found that the stimulation of NMDA receptor by glycine treatment for LTP induction stimulated SynGAP1 phosphorylation, Ras-ERK activation, spine enlargement and SynGAP1 delocalization from the spines in striatal neurons, and these effects were prevented by Rho-kinase inhibition. Rho-kinase-mediated phosphorylation of SynGAP1 appeared to increase its dissociation from PSD95, a postsynaptic scaffolding protein located at postsynaptic density, by forming a complex with 14-3-3ζ. These results suggest that Rho-kinase phosphorylates SynGAP1 at Ser842, thereby activating the Ras-ERK pathway for NMDA-induced morphological changes in dendritic spines.

Keywords SynGAP1 · Rho-kinase · Ras · Phosphorylation · Long-term potentiation · Dendritic spine

Introduction

Glutamate is the most abundant excitatory neurotransmitter and acts through ionotropic receptors, including AMPA receptors (AMPA-R), NMDA receptors (NMDA-R) and Kainate receptors [1–3]. When glutamate binds to AMPA-R at the postsynaptic membranes, Na^+ flows into the postsynaptic cells and subsequently induces depolarization. NMDA-R is thought to play important roles in controlling long-term potentiation (LTP), which is one of the most investigated synaptic plasticity and is important for establishing memory, learning, activity-dependent development, and other higher brain processes [4, 5]. Under the depolarized state induced by AMPA-R activation, glutamate stimulates the influx of Ca^{2+} into postsynaptic cells through NMDA-R, which is followed by activating CaMKII and then promoting AMPA-R trafficking via presynaptic sites or intracellular pools to the postsynaptic density for LTP. Ras-ERK signaling is also required for AMPA-R trafficking and surface delivery following LTP induction [6, 7].

One of the key features of LTP is structural synaptic plasticity, such as dendritic spine enlargements [8]. Upon stimulation of NMDA-R, CaMKII is thought to activate RhoA and its effector Rho-kinase/ROCK for spine enlargement, presumably through promoting actin polymerization [9–11]. The Ras-ERK pathway is also involved in spine enlargement during NMDA-dependent LTP [12]. However, the regulatory interaction between RhoA-Rho-kinase and Ras underlying spine enlargement and LTP is still largely unknown.

Mengya Wu and Yasuhiro Funahashi have contributed equally.

✉ Kozo Kaibuchi
kaibuchi@fujita-hu.ac.jp

1 Department of Cell Pharmacology, Nagoya University Graduate School of Medicine, Nagoya 466-8550, Japan

2 International Center for Brain Science, Fujita Health University, Toyoake, Aichi 470-1129, Japan

3 Department of Physiology, Keio University School of Medicine, Tokyo 160-8582, Japan

4 PRESTO-JST, Kawaguchi, Saitama 332-0012, Japan

5 Department of Neuropsychopharmacology and Hospital Pharmacy, Nagoya University Graduate School of Medicine, Nagoya, Aichi, Japan

Published online: 27 May 2022

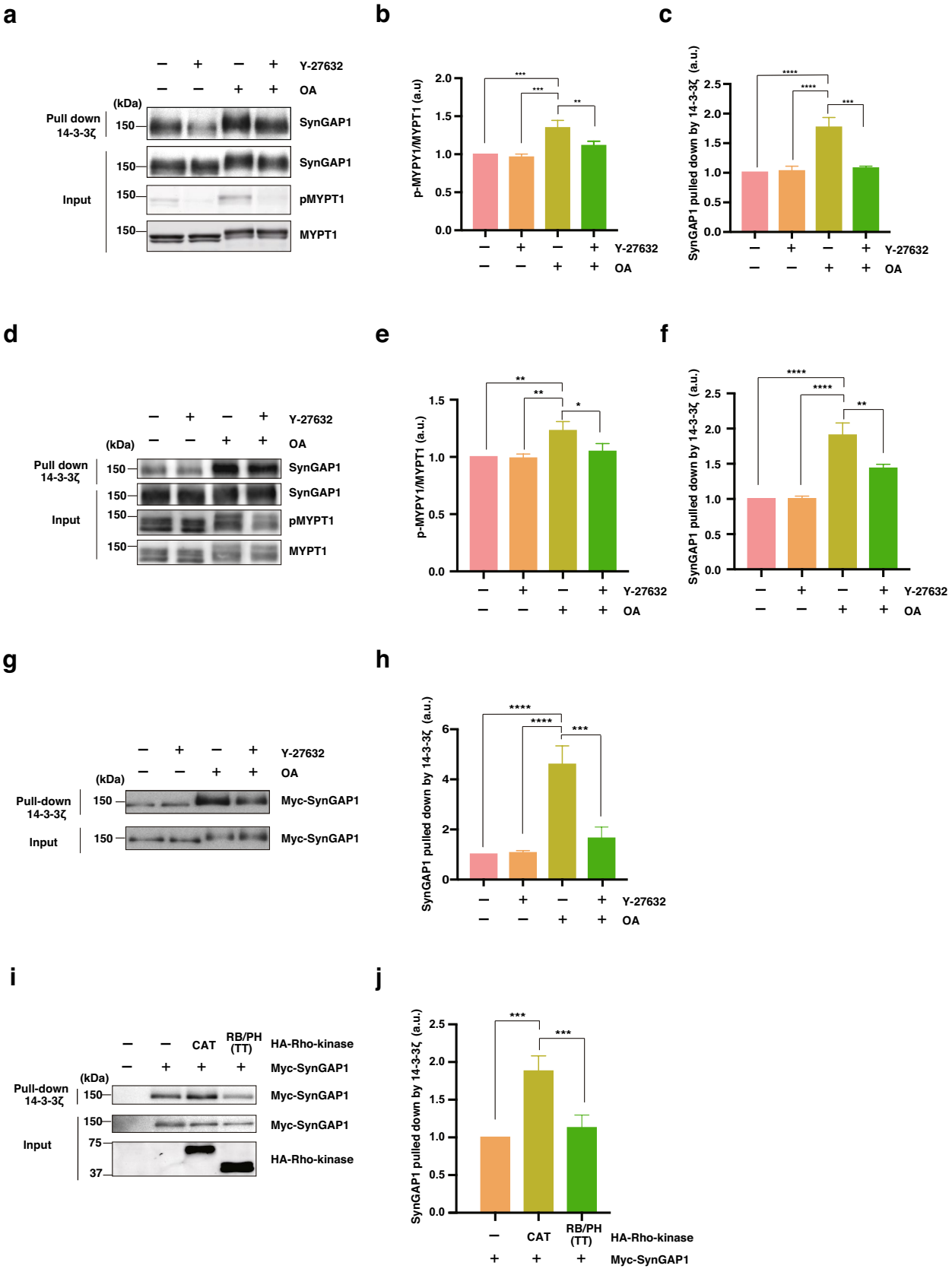
a
Y-27632
OA
(kDa)
Pull down 14-3-3ζ
150
SynGAP1
Input
150
SynGAP1
150
pMYPT1
150
MYPT1
b
p-MYPY1/MYPT1 (a.u)
2.0
1.5
1.0
0.5
0.0
***
***
**
Y-27632
OA
c
SynGAP1 pulled down by 14-3-3ζ (a.u.)
2.5
2.0
1.5
1.0
0.5
0.0
****
****
***
Y-27632
OA
d
Y-27632
OA
(kDa)
Pull down 14-3-3ζ
150
SynGAP1
Input
150
SynGAP1
150
pMYPT1
150
MYPT1
e
p-MYPY1/MYPT1 (a.u.)
1.5
1.0
0.5
0.0
**
**
*
Y-27632
OA
f
SynGAP1 pulled down by 14-3-3ζ (a.u.)
2.5
2.0
1.5
1.0
0.5
0.0
****
****
**
Y-27632
OA
g
Y-27632
OA
(kDa)
Pull-down 14-3-3ζ
150
Myc-SynGAP1
Input
150
Myc-SynGAP1
h
SynGAP1 pulled down by 14-3-3ζ (a.u.)
6
4
2
0
****
****
***
Y-27632
OA
i
CAT
RB/PH (TT)
HA-Rho-kinase
Myc-SynGAP1
(kDa)
Pull-down 14-3-3ζ
150
Myc-SynGAP1
Input
150
Myc-SynGAP1
75
37
HA-Rho-kinase
j
SynGAP1 pulled down by 14-3-3ζ (a.u.)
2.5
2.0
1.5
1.0
0.5
0.0
***
***
CAT
RB/PH (TT)
HA-Rho-kinase
Myc-SynGAP1

◂**Fig. 1** Rho-kinase regulates the interaction of SynGAP1 with 14-3-3ζ. **a** Rho-kinase regulates the interaction of SynGAP1 with 14-3-3ζ in cultured striatal neurons. Cultured striatal neurons were treated with DMSO or Y-27632 (20 μM) for 1 h and then stimulated with okadaic acid (OA, 1 μM) for 1 h followed by pulldown with affinity beads coated with GST-14-3-3ζ. Samples were analyzed by immunoblotting with anti-SynGAP1, anti-pMYPT1 (S853) and anti-MYPT1 antibodies. **b** The bar graph shows the relative intensity of pMYPT1 normalized to total MYPT1. Data represent the mean ± SEM of three independent experiments and were analyzed by one-way ANOVA with Tukey's post hoc test. **P < 0.01. ***P < 0.001. **c** The bar graph shows the amounts of SynGAP1 pulled down by GST-14-3-3ζ. Data represent the mean ± SEM of four independent experiments and were analyzed by one-way ANOVA with Tukey's post hoc test. ***P < 0.001. ****P < 0.0001. **d** Striatal slices were treated with DMSO or Y-27632 (20 μM) for 1 h and then stimulated with okadaic acid (OA, 1 μM) for 1 h followed by pulldown with affinity beads coated with GST-14-3-3ζ. Samples were analyzed by immunoblotting with anti-SynGAP1, anti-pMYPT1 (S853) and anti-MYPT1 antibodies. **e** The bar graph shows the relative intensity of pMYPT1 normalized to total MYPT1. Data represent the mean ± SEM of four independent experiments and were analyzed by one-way ANOVA with Tukey's post hoc test. *P < 0.05. **P < 0.01. **f** The bar graph shows the amounts of SynGAP1 pulled down by GST-14-3-3ζ. Data represent the mean ± SEM of four independent experiments and were analyzed by one-way ANOVA with Tukey's post hoc test. **P < 0.05. ****P < 0.0001. **g** Rho-kinase regulates the interaction of SynGAP1 with 14-3-3ζ in HeLa cells. HeLa cells were transfected with Myc-SynGAP1-WT, treated with DMSO or Y-27632 (20 μM) for 1 h and stimulated with okadaic acid (OA, 1 μM) for 1 h followed by pulldown with affinity beads coated with GST-14-3-3ζ. Samples were analyzed by immunoblotting with an anti-Myc antibody. **h** The bar graph shows the amounts of SynGAP1 pulled down by GST-14-3-3ζ. Data represent the mean ± SEM of four independent experiments and were analyzed by one-way ANOVA with Tukey's post hoc test. ***P < 0.001. ****P < 0.0001. **i** HeLa cells were cotransfected with Myc-SynGAP1-WT and HA-Rho-kinase-CAT or -RB/PH (TT) followed by pulldown with affinity beads coated with GST-14-3-3ζ. Samples were analyzed by immunoblotting with anti-Myc and anti-HA antibodies. **j** The bar graph shows the amounts of SynGAP1 pulled down by GST-14-3-3ζ. Data represent the mean ± SEM of four independent experiments and were analyzed by one-way ANOVA with Tukey's post hoc test. ***P < 0.001

We previously developed a novel phosphoproteomic method called phosphatase inhibitor and kinase inhibitor substrate screening (PIKISS) that could comprehensively identify Rho-kinase substrates [13, 14]. Briefly, HeLa cells were treated with a phosphatase inhibitor (calyculin A) and/or Rho-kinase inhibitor (Y-27632). Calyculin A treatment induced the phosphorylation of large numbers of proteins, including Rho-kinase substrates, and pretreatment with Y-27632 specifically inhibited Rho-kinase-mediated phosphorylation. The cell lysates containing Rho-kinase substrates were pulled down by beads coated with 14-3-3ζ, which specifically interacted with phosphorylated proteins [15], to enrich phosphoproteins. The bound proteins were subjected to tryptic digestion and LC–MS/MS to identify the phosphorylated proteins and their phosphorylation sites. The comparison between the treatments with calyculin A and with calyculin A and Y-27632 identified more than one hundred Rho-kinase substrate candidates, including known substrates such as MYPT1 [16]. The data obtained from the phosphoproteomics were registered on the online database named KANPHOS (kinase-associated neural phospho-signaling), which we developed and published [17–19] (https://kanphos.neuroinf.jp). KANPHOS provides the phosphorylated proteins and sites identified by the above mentioned approach as well as those previously reported in the literature. We registered similar data that was obtained from striatum neurons. We hypothesized that the KANPHOS data contained Rho-kinase substrate candidates that regulated Ras activity, performed pathway analysis, and identified SynGAP1 as a candidate. SynGAP1 (Synaptic Ras-GTPase-activating protein) converts the GTP-bound active form of Ras to the GDP-bound inactive form [20–22]. SynGAP1 is involved in synaptic plasticity, AMPA-R trafficking to the postsynaptic membrane and ERK activity [23–26].

Considering these observations, we examined whether Rho-kinase phosphorylated SynGAP1 and found that Rho-kinase phosphorylated SynGAP1 and increased its interaction with 14-3-3ζ, thereby stimulating the Ras-ERK pathway for the structural plasticity of dendritic spines in striatum neurons.

Results

The Interaction of SynGAP1 with 14-3-3ζ is Regulated by Rho-Kinase

The KANPHOS database predicted that Rho-kinase phosphorylated SynGAP1 and increased its association with 14-3-3. We first examined whether 14-3-3 interacts endogenously with SynGAP1 in vivo and which isoforms of 14-3-3 (β, γ, ε, η, σ, θ and ζ) interact with SynGAP1 by immunoprecipitation assay. When SynGAP1 was immunoprecipitated from mouse striatum lysate, 14-3-3γ, 14-3-3ε and 14-3-3ζ were coprecipitated, but 14-3-3β, 14-3-3η, 14-3-3σ and 14-3θ were not (Fig. S1). These results suggest that SynGAP1 interacts with 14-3-3γ, 14-3-3ε, and 14-3-3ζ in vivo. 14-3-3ε and 14-3-3ζ have been implicated in several neuropsychiatric diseases, including autism spectrum disorder and schizophrenia [27–30]. Furthermore, it has been reported that 14-3-3ζ knockout mice show reduced spine density [31] and overexpression of 14-3-3ζ in cultured neurons promotes spine formation [32]. Therefore, we focused on 14-3-3ζ in subsequent experiments. Next, to examine whether Rho-kinase regulates the interaction of SynGAP1 with 14-3-3ζ, cultured striatal neurons were incubated with DMSO or Y-27632 for 1 h and subsequently treated with okadaic acid, a phosphatase inhibitor, for 1 h. The cell lysates were analyzed by immunoblotting with an antibody against phosphorylated MYPT1 (T853), which is the specific

substrate of Rho-kinase (Fig. 1a, b) [16, 33]. Okadaic acid induced MYPT1 phosphorylation, and this phosphorylation was prevented by Y-27632 (Fig. 1a, b), indicating that Rho-kinase-mediated phosphorylation is induced by okadaic acid in neurons and that phosphorylation is blocked by Y-27632. The rest of the cell lysates were subjected to a pulldown assay using affinity beads coated with GST-14-3-3ζ to capture phosphorylated proteins and immunoblotting with the anti-SynGAP1 antibody. Okadaic acid increased the interaction of SynGAP1 with 14-3-3ζ, whereas Y-27632 reduced the okadaic acid-induced interaction (Fig. 1a, c).

We next performed similar experiments ex vivo by using striatal slice cultures. The striatal slices were cultured and treated with DMSO or Y-27632 for 1 h and then stimulated with okadaic acid for 1 h. Treatment with okadaic acid increased the binding of SynGAP1 to 14-3-3ζ, whereas this increase was prevented by treatment with Y-27632 (Fig. 1d–f). We confirmed the above results using the reconstitution systems in HeLa cells. The plasmid harboring Myc-SynGAP1 was transfected into HeLa cells. Twenty-four hours after transfection, the cells were treated with DMSO or Y-27632 for 1 h and then incubated with okadaic acid for 1 h. The cell extracts were applied to affinity beads coated with GST-14-3-3ζ, followed by immunoblot analysis using the anti-Myc antibody. Treatment of the cells with okadaic acid increased Myc-SynGAP1 binding to 14-3-3ζ, but this increase was reversed by pretreatment with Y-27632 (Fig. 1g, h). We next cotransfected plasmids harboring Myc-SynGAP1 with the constitutively active form of Rho-kinase (HA-Rho-kinase-CAT) or the dominant negative form of Rho-kinase (HA-Rho-kinase-RB/PH (TT)) into HeLa cells for the pulldown assay. Coexpression of Rho-kinase-CAT with Myc-SynGAP1 increased the binding of Myc-SynGAP1 to 14-3-3ζ, whereas coexpression of HA-Rho-kinase-RB/PH (TT) with Myc-SynGAP1 did not increase it (Fig. 1 i, j). Thus, Rho-kinase positively regulates the interaction of SynGAP1 with 14-3-3ζ.

14-3-3ζ, Interacts with the C-Terminal Domain of SynGAP1

To narrow down the binding site of SynGAP1 to 14-3-3ζ, we prepared three fragments of SynGAP1 named SynGAP1-NT (1–442 aa), NTMD (1–784 aa) and CT (785–1343 aa) (Fig. 2a). SynGAP1-NT contains the PH and C2 domains. SynGAP1-NTMD covers the PH, C2 and RasGAP domains, and SynGAP1-CT contains the disordered and CC domains. Plasmids harboring Myc-SynGAP1-NT, Myc-SynGAP1-NTMD or Myc-SynGAP1-CT were transfected into HeLa cells. The cells were treated with DMSO or Y-27632 for 1 h and then stimulated with okadaic acid for 1 h. The cell extracts were analyzed by immunoblotting with the anti-Myc antibody (Fig. 2b). Okadaic acid increased the interaction of Myc-SynGAP1-CT with 14-3-3ζ, whereas Y-27632 reduced this interaction (Fig. 2e). Okadaic acid appears to slightly increase the binding of Myc-SynGAP1-NT or Myc-SynGAP1-NTMD to 14-3-3ζ, but the difference was not statistically significant (Fig. 2c, d). Although there may be multiple 14-3-3 binding sites within SynGAP1, the present results suggest that Rho-kinase enhances the interaction between SynGAP1 and 14-3-3ζ mainly through the C-terminal domain of SynGAP1.

Rho-Kinase Phosphorylates SynGAP1 at Ser842

To examine whether Rho-kinase directly phosphorylates SynGAP1, we performed an in vitro kinase assay using SynGAP1 fragments (GST-SynGAP1-NT, GST-SynGAP1-NTMD, and GST-SynGAP1-CT). The plasmids encoding GST-SynGAP1-NT, NTMD or CT were transfected into COS7 cells, and the GST-fusion proteins were purified by glutathione affinity beads. GST-SynGAP1-NT, NTMD or CT was incubated with Rho-kinase-CAT in the presence of [γ- ^{32}P]ATP. SynGAP1-CT was efficiently phosphorylated by Rho-kinase, whereas SynGAP1-NT and SynGAP1-NTMD were weakly phosphorylated (Fig. 3a, b). The KANPHOS data predicted that Rho-kinase phosphorylated SynGAP1 at Ser842 in the C-terminal disorganized domain.

To examine whether Rho-kinase phosphorylates SynGAP1 at Ser842, we generated a specific antibody against the SynGAP1 phosphorylated at Ser842 (anti-pS842 SynGAP1 antibody). We next examined whether Rho-kinase phosphorylated SynGAP1 in intact cells. The plasmids harboring Myc-SynGAP1 were transfected into HeLa cells, and the cells were treated with DMSO or Y-27632 for 1 h and then stimulated with okadaic acid for 1 h. Immunoblot analysis with anti-p842 SynGAP1 and anti-Myc antibodies revealed that okadaic acid induced SynGAP1 phosphorylation at Ser842 and Y-27632 prohibited it (Fig. 3c, d). To further explore the role of Rho-kinase, we expressed HA-Rho-kinase-CAT or RB/PH (TT) with Myc-SynGAP1 in HeLa cells. The expression of Rho-kinase-CAT increased SynGAP1 phosphorylation at Ser842, but RB/PH (TT) did not stimulate it (Fig. 3e, f). Because Ser842 is located in the 14-3-3 binding region in SynGAP1, we compared the binding of SynGAP1 and 14-3-3ζ with that of SynGAP1-S842A, in which Ser842 was substituted for Ala, and found that Ala substitution of Ser842 reduced the binding activity to 14-3-3ζ (Fig. 3g, h). These results indicate that Rho-kinase phosphorylates SynGAP1 at Ser842 and positively regulates the interaction of SynGAP1 with 14-3-3ζ.

Phosphorylation of SynGAP1 by Rho-Kinase Regulates Ras and ERK Activity

Because SynGAP1 is a negative regulator of Ras and the binding of 14-3-3 usually affects the binding partner's

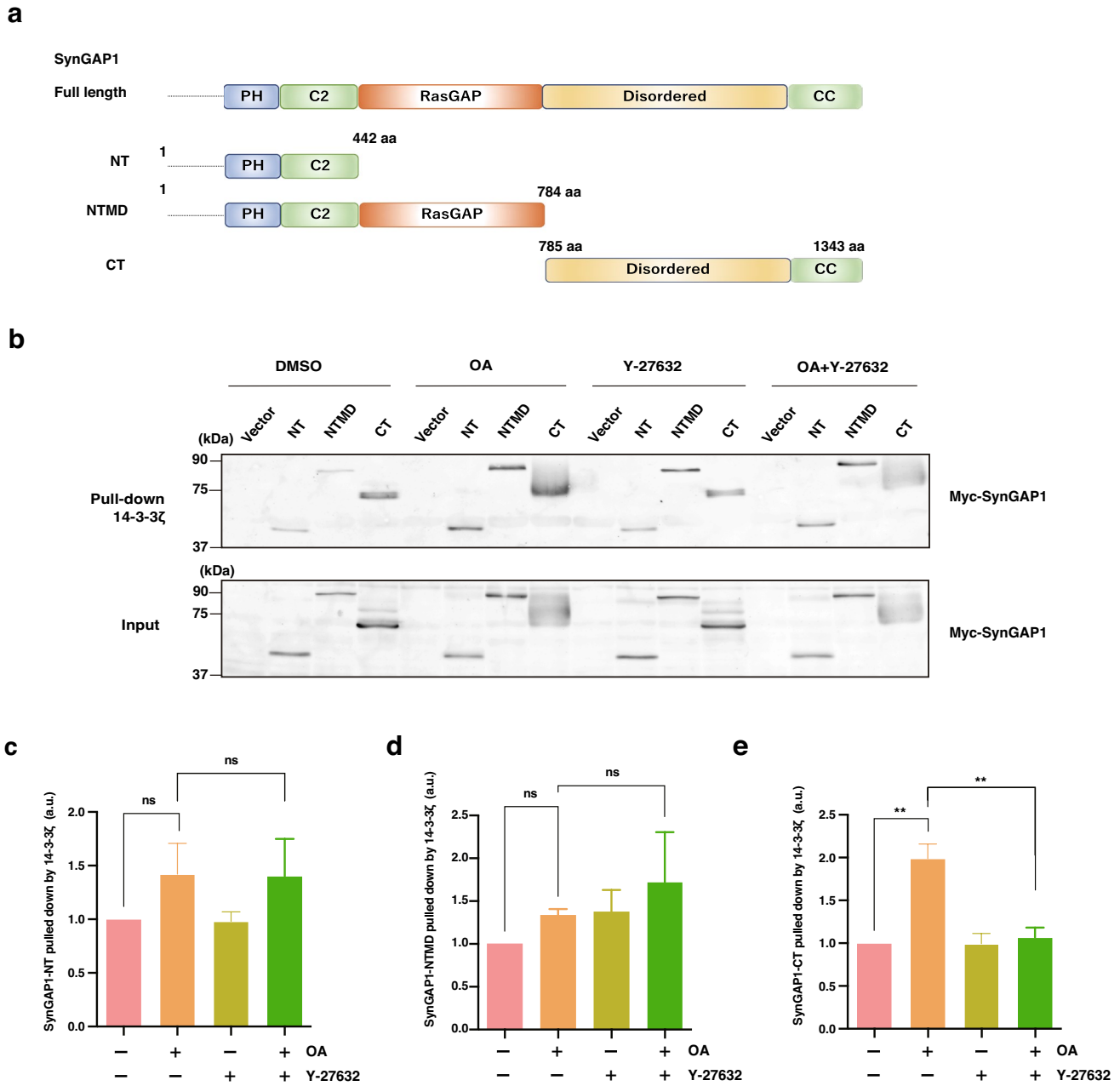

Fig. 2 Identification of the phosphorylation site of SynGAP1 by Rho-kinase. **a** Representation of the domain structures of SynGAP1 and its various fragments. SynGAP1 contains the Pleckstrin Homology (PH) domain, C2 domain, RasGAP domain, disordered domain and coiled-coil (CC) domain. **b** Rho-kinase regulates the interaction of the C-terminus of SynGAP1 with 14-3-3ζ in HeLa cells. SynGAP1-NT, SynGAP1-NTMD or SynGAP1-CT was transfected into HeLa cells, treated with Y-27632 (20 μM) and/or OA (1 μM) for 1 h, and then pulled down by GST-14-3-3ζ. Samples were analyzed by immunoblotting with an anti-Myc antibody. **c** The bar graph shows the amounts of SynGAP1-NT pulled down by GST-14-3-3ζ. Data represent the mean ± SEM of three independent experiments and were analyzed by one-way ANOVA with Tukey's post hoc test. ns: not significant. **d** The bar graph shows the amounts of SynGAP1-NTMD pulled down by GST-14-3-3ζ. Data represent the mean ± SEM of three independent experiments and were analyzed by one-way ANOVA with Tukey's post hoc test. ns: not significant. **e** The bar graph shows the amounts of SynGAP1-CT pulled down by GST-14-3-3ζ. Data represent the mean ± SEM of three independent experiments and were analyzed by one-way ANOVA with Tukey's post hoc test. $^{**}P < 0.01$

activity, we next investigated whether Rho-kinase regulates Ras activity through SynGAP1 phosphorylation. HA-Rho-kinase-CAT or RB/PH (TT) was expressed with Myc-SynGAP1 in HeLa cells. The cell lysates were incubated with GST-Raf1-RBD to precipitate active Ras, which was followed by immunoblot analysis using anti-Ras and

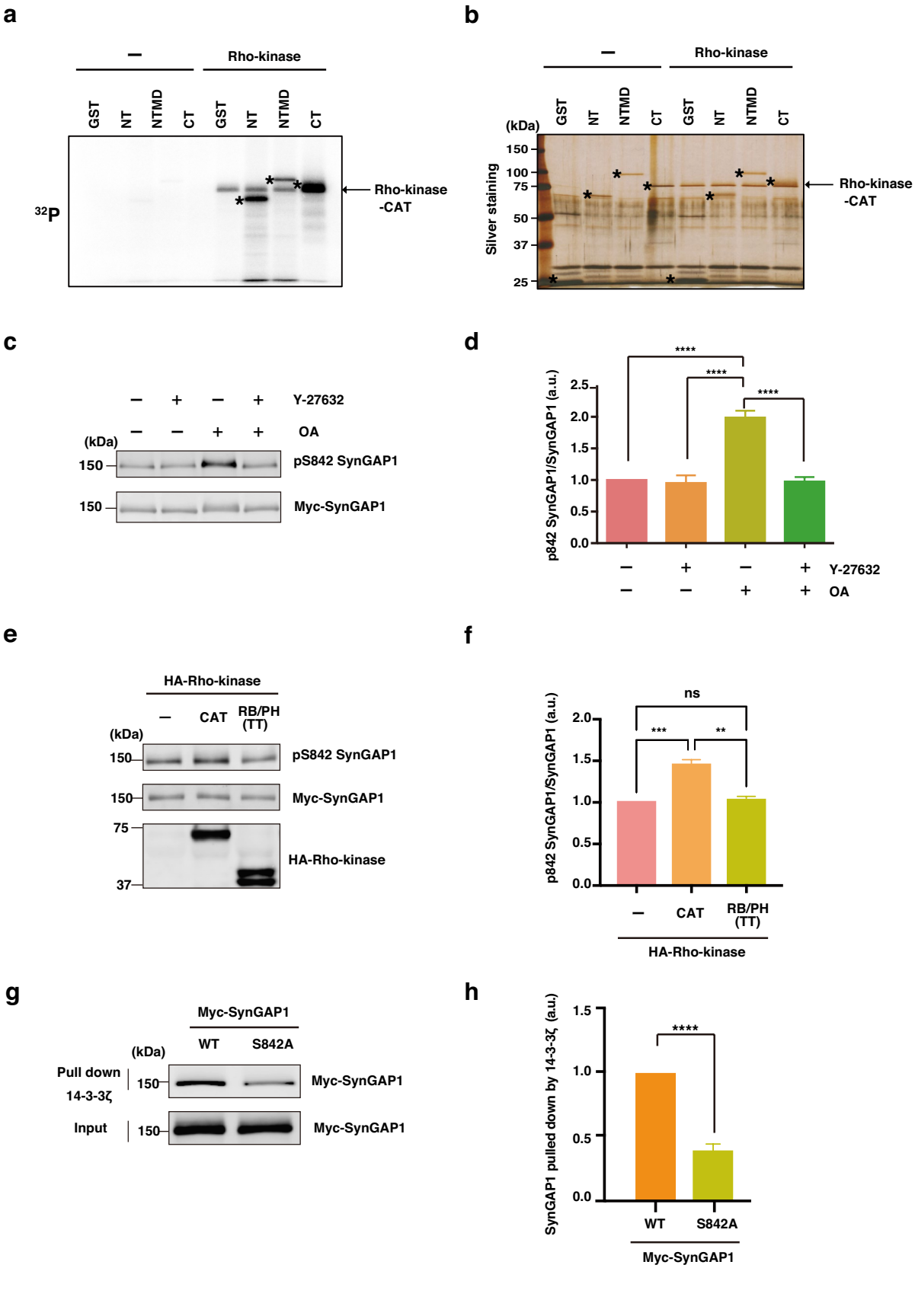
a
–
Rho-kinase
GST
NT
NTMD
CT
GST
NT
NTMD
CT
32P
Rho-kinase
-CAT
b
–
Rho-kinase
GST
NT
NTMD
CT
GST
NT
NTMD
CT
(kDa)
150
100
75
50
37
25
Silver staining
Rho-kinase
-CAT
c
–
+
–
+
Y-27632
–
–
+
+
OA
(kDa)
150
pS842 SynGAP1
150
Myc-SynGAP1
d
****
****
****
p842 SynGAP1/SynGAP1 (a.u.)
2.5
2.0
1.5
1.0
0.5
0.0
–
+
–
+
Y-27632
–
–
+
+
OA
e
HA-Rho-kinase
–
CAT
RB/PH
(TT)
(kDa)
150
pS842 SynGAP1
150
Myc-SynGAP1
75
37
HA-Rho-kinase
f
ns
***
**
p842 SynGAP1/SynGAP1 (a.u.)
2.0
1.5
1.0
0.5
0.0
–
CAT
RB/PH
(TT)
HA-Rho-kinase
g
Myc-SynGAP1
WT
S842A
(kDa)
Pull down
14-3-3ζ
150
Myc-SynGAP1
Input
150
Myc-SynGAP1
h
****
SynGAP1 pulled down by 14-3-3ζ (a.u.)
1.5
1.0
0.5
0.0
WT
S842A
Myc-SynGAP1

◂**Fig. 3** Rho-kinase phosphorylate SynGAP1 at Ser842. **a**, **b** The direct phosphorylation of SynGAP1 by Rho-Kinase. GST-SynGAP1 fragments were transfected into COS7 cells, and GST-SynGAP1 fragments were purified by Glutation Sepharose 4B beads. Purified GST-SynGAP1 fragments were incubated with or without GST-Rho-kinase-CAT (50 nM) in the presence of [γ- ^{32}P] ATP at 30 °C for 20 min. Samples were subjected to SDS-PAGE and silver staining followed by autoradiography. Asterisks indicate intact GST-SynGAP1 fusion proteins. Arrow indicates recombinant Rho-kinase-CAT. **c** Myc-SynGAP1-WT was transfected into HeLa cells and stimulated with Y-27632 (20 μM) and OA (1 μM) for 1 h. Samples were analyzed by immunoblotting with anti-pS842-SynGAP1 and anti-Myc antibodies. **d** The bar graph shows the relative intensity of pSynGAP1 (S842) normalized to total SynGAP1. Data represent the mean ± SEM of four independent experiments and were analyzed by one-way ANOVA with Tukey's post hoc test. ****P < 0.0001. **e** Myc-SynGAP1-WT and HA-Rho-kinase-CAT or -RB/PH (TT) were transfected into HeLa cells. Samples were analyzed by immunoblotting with anti-pS842-SynGAP1, anti-Myc and anti-HA antibodies. **f** The bar graph shows the relative intensity of pSynGAP1 (S842) normalized to total SynGAP1. Data represent the mean ± SEM of four independent experiments and were analyzed by one-way ANOVA with Tukey's post hoc test. ***P < 0.001, **P < 0.01. ns: not significant. **g** The S842A mutant of SynGAP1 decreased the interaction with 14-3-3ζ. HeLa cells were transfected with Myc-SynGAP1-WT or S842A, which was followed by pulldown with affinity beads coated with 14-3-3ζ. The samples were analyzed by immunoblotting with an anti-Myc antibody. **h** The bar graph shows the amounts of SynGAP1 pulled down by 14-3-3ζ. Data represent the mean ± SEM of three independent experiments and were analyzed by one-way ANOVA with Tukey's post hoc test. ****P < 0.0001

phosphorylated ERK (active ERK) (Fig. 4a–c). The activity of Ras and ERK1/2 phosphorylation were significantly decreased when only SynGAP1 was expressed (Fig. 4a–c). Coexpression of Rho-kinase-CAT with SynGAP1 increased active Ras and ERK1/2 phosphorylation, but neither were stimulated with that of RB/PH (TT) (Fig. 4a–c). Under the same conditions, Rho-kinase-CAT did not show the stimulatory effect of SynGAP1-S842A on Ras activity and ERK phosphorylation (Fig. 4d–f), suggesting that Rho-kinase phosphorylates SynGAP1 at Ser842, thereby stimulating Ras-ERK signaling.

Chemical LTP Regulates Ras and ERK Activity Through Rho-Kinase-SynGAP1

To examine whether Rho-kinase regulates the Ras-ERK pathway through SynGAP1 phosphorylation in neurons, we prepared DIV21 striatal neurons and then chemically induced LTP using a standard protocol that selectively activated synaptic NMDARs (Chemical LTP). In this method, magnesium in the media was withdrawn in conjunction with glycine perfusion. With spontaneous glutamate release from axonal terminals, glycine strongly and specifically stimulates synaptic NMDARs [34–37]. The striatal neurons were treated with DMSO or Y-27632 for 1 h and then incubated with glycine to induce chemical LTP for 10 min or 60 min, which was followed by morphology analysis of dendritic spines using anti-SynGAP1 and PSD95 antibodies (Fig. 5a). PSD95 is a membrane-associated guanylate kinase scaffolding protein located in postsynaptic densities [38, 39]. SynGAP1 is localized at dendritic spines and forms a large macromolecule complex with PSD95 and NMDA-R [21]. We found that treatment with glycine induced a sustained increase in dendritic spine size at 10 min and 60 min (Fig. 5b), as previously described [26]. We also found that glycine treatment showed a decrease in SynGAP1 colocalized with PSD95 at the spines (Fig. 5c). However, pretreatment with Y-27632 inhibited the glycine-induced increases in spine size and dispersion of SynGAP1 from the spines (Fig. 5 b, c).

We next examined whether chemical LTP induction modulated the interactions among SynGAP1, PSD95 and 14-3-3ζ. After treatment with glycine, SynGAP1 was immunoprecipitated from the cell lysates with the anti-SynGAP1 antibody, and the immunoprecipitants were subjected to immunoblot analysis with the anti-PSD95 and anti-14-3-3ζ antibodies (Fig. 5d–f). The amounts of PSD95 immunoprecipitated with SynGAP1 progressively decreased during chemical LTP, whereas those of 14-3-3ζ increased (Fig. 5e, f). These changes were reversed by pretreating the neurons with Y-27632 (Fig. 5e, f). We also tested whether SynGAP1 was phosphorylated during chemical LTP using the anti-p842 SynGAP1 antibody but could not detect phosphorylation. This failure may be due to the low sensitivity of the antibody and expression levels of SynGAP1. However, we assume that chemical LTP induction stimulates SynGAP1 phosphorylation by Rho-kinase because treatment with glycine increased the interaction of SynGAP1 with 14-3-3ζ and pretreatment with Y-27632 inhibited the interaction (Fig. 5d, f). We examined whether chemical LTP induction affected Ras-ERK signaling. After treatment with glycine, we measured the Ras activity and the phosphorylation of MYPT1 and ERK. The results showed that glycine treatment stimulated Ras activity and the phosphorylation of MYPT1 and ERK in a time-dependent manner, and these effects were prevented by pretreatment with Y-27632 (Fig. 5g–j).

To further explore the relationship among SynGAP1, PSD95 and 14-3-3ζ, we cotransfected plasmids harboring Myc-SynGAP1, EGFP-PSD95, and GST-14-3-3ζ into HeLa cells. The transfected cells were treated with DMSO or Y-27632 for 1 h and then incubated with okadaic acid for 1 h. Myc-SynGAP1 was immunoprecipitated with the anti-Myc antibody, and the immunoprecipitants were analyzed by immunoblotting with the anti-Myc, anti-EGFP, anti-GST, anti-MYPT1 and anti-pMYPT1 antibodies (Fig. 6a–e). Treatment with okadaic acid increased MYPT1 phosphorylation and the association of Myc-SynGAP1 with GST-14-3-3ζ and decreased the association with EGFP-PSD95, whereas the effects of okadaic acid were negated by

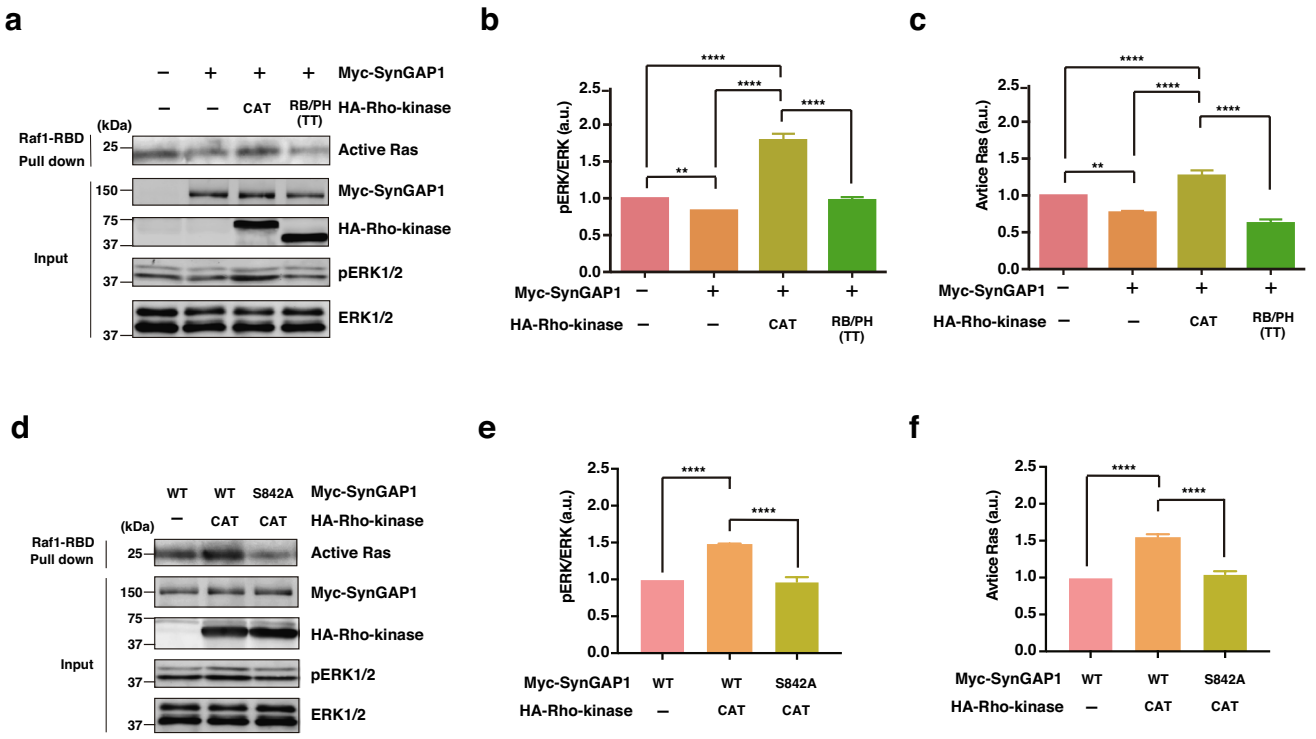

Fig. 4 Phosphorylation of SynGAP1 by Rho-kinase regulates Ras and ERK activity. **a** HA-Rho-kinase-CAT or -RB/PH (TT) and Myc-SynGAP1 were transfected into HeLa cells. Cell lysates were incubated with GST-Raf1-RBD to precipitate active Ras, followed by immunoblotting with anti-Ras, anti-Myc, anti-HA, anti-pERK1/2, and anti-ERK1/2 antibodies. **b** The bar graph shows the relative intensity of pERK1/2 normalized to total ERK1/2. Data represent the mean ± SEM of nine independent experiments and were analyzed by one-way ANOVA with Tukey's post hoc test. **P < 0.01, ****P < 0.0001. **c** The bar graph shows amounts of active Ras. Data represent the mean ± SEM of nine independent experiments and were analyzed by one-way ANOVA with Tukey's post hoc test. **P < 0.01, ****P < 0.0001. **d** HA-Rho-kinase-CAT was cotransfected with Myc-SynGAP1-WT or -S842A into HeLa cells. Cell lysates were incubated with GST-Raf1-RBD to precipitate active Ras, followed by immunoblotting with anti-Ras, anti-Myc, anti-HA, anti-pERK1/2, and anti-ERK1/2 antibodies. **e** The bar graph shows the relative intensity of pERK1/2 normalized to total ERK1/2. Data represent the mean ± SEM of three independent experiments and were analyzed by one-way ANOVA with Tukey's post hoc test. ****P < 0.0001. **f** The bar graph shows amounts of active Ras. Data represent the mean ± SEM of three independent experiments and were analyzed by one-way ANOVA with Tukey's post hoc test. ****P < 0.0001

pretreatment with Y-27632 (Fig. 6a–e). These results suggest that Rho-kinase increases the interaction of SynGAP1 with 14-3-3ζ and decreases the interaction with PSD95.

Discussion

Brief Summary and Conclusion

Stimulation of NMDA-R to induces RhoA activation through Ca^{2+}-CaMKII signaling [9]. In this study, we found that Rho-kinase phosphorylated SynGAP1 at Ser842 and induced the association of SynGAP1 with 14-3-3ζ, thereby activating Ras-ERK signaling (Fig. 1–4). The stimulation of NMDA-R by glycine treatment for LTP induction stimulated SynGAP1 phosphorylation, Ras-ERK activation, spine enlargement and delocalization of SynGAP1 from the spines in striatal neurons, whereas these effects were prevented by pretreatment with a Rho-kinase inhibitor (Y-27632). The Rho-kinase-mediated phosphorylation of SynGAP1 appeared to induce its dissociation from PSD95 but its association with 14-3-3 (Fig. 6a–e). Based on our findings with previous findings, we propose the mechanism by which the RhoA-Rho-kinase signal regulates Ras-ERK signaling during LTP induction (Fig. 6f). Upon NMDA-R stimulation, the influx of Ca^{2+} to neurons is induced to activate CaMKII, thereby stimulating RhoA-Rho-kinase. Rho-kinase phosphorylates SynGAP1 and induces its association with 14-3-3ζ, resulting in inactivation of SynGAP1 activity and its dissociation from PSD95, which is anchored to NMDA-R. Eventually, Ras-ERK signaling is activated, leading to postsynaptic insertion of AMPA-R and spine enlargement, as previously reported [12]. On the other hand, the RhoA-Rho-kinase pathway appears to modulate actin polymerization, resulting in spine enlargement (Fig. 6f).

SynGAP1 is a Novel Rho-Kinase Substrate

It has been reported that SynGAP1 is phosphorylated by PLK2, CDK5, and CaMKII [26, 40, 41]. SynGAP1 is phosphorylated on the C-terminal side of its GAP domain by PLK2, which increases the Ras-GAP activity of SynGAP1 [41]. CDK5 phosphorylates SynGAP1 at Ser773 and Ser802. Phosphorylation of SynGAP1 at Ser773 inhibits Ras-GAP activity, and phosphorylation at Ser802 increases it [40]. CaMKII phosphorylates SynGAP1 at Ser1108 and Ser1138 and inhibits binding of SynGAP1 to PSD95[26]. We also confirmed that ectopic expression of constitutive active CaMKII in COS7 cells inhibits the interaction of SynGAP1 with PSD95 (Fig. S2) The phosphorylation of SynGAP1 by CaMKII during LTP induction in hippocampal neurons results in rapid dispersion of SynGAP1 from the spine and activation of Ras-ERK signals in the spine [26]. In this study, we found that Rho-kinase directly phosphorylates SynGAP1 at Ser842 and inhibits the interaction of SynGAP1 with PSD95. A Rho-kinase inhibitor (Y-27632) suppressed the activation of Ras and ERK during LTP induction in striatal neurons (Fig. 5g–j), suggesting that Rho-kinase plays an important role in Ras-ERK signaling downstream of NMDA-R. It has been reported that NMDA-R stimulation induces the influx of Ca^{2+} into neurons, activating CaMKII, which in turn activates the RhoA-Rho-kinase pathway [9]. Thus, it is suggested that SynGAP1 is sequentially phosphorylated by CaMKII and Rho-kinase downstream of NMDA-Rs during LTP induction, and consequently SynGAP1 deviates from the spine and activates Ras-ERK signaling.

Rho-kinase Regulates Ras-ERK Signaling via Phosphorylation of SynGAP1

We found that the activation of Rho-kinase phosphorylated SynGAP1 and promoted the activation of Ras-ERK signaling in Raf-RBD pulldown experiments (Fig. 4a–c). Additionally, stimulation of NMDA-R with glycine to induce LTP promoted the activation of Ras-ERK in striatal neurons, and these effects were prevented by pretreatment with a Rho-kinase inhibitor (Y-27632) (Fig. 5g–j). Thus, it was suggested that Rho-kinase inhibits the GAP activity of SynGAP1. However, there is no evidence that Rho-kinase directly regulates the GAP activity of SynGAP1. We consider two possibilities. We found that phosphorylation by Rho-kinase induced the binding of SynGAP1 to 14-3-3ζ (Fig. 1a–j). We also showed that the SynGAP1-S842A mutant suppressed the activation of Ras-ERK signaling by Rho-kinase (Fig. 4 d–f). Therefore, phosphorylation of SynGAP1 may inhibit GAP activity when it binds to 14-3-3ζ. We also found that the phosphorylation of SynGAP1 by Rho-kinase inhibited the binding of SynGAP1 to PSD95 (Fig. 6a–e). SynGAP1 dissociated from PSD95 in striatal neuronal spines when NMDA-R was stimulated with glycine to induce LTP (Fig. 5a–f). Thus, it is likely that phosphorylated SynGAP1 interacts with 14-3-3ζ to change the conformation of SynGAP1, and this conformational change also dissociates SynGAP1 from PSD95.

Experimental Procedures

Animals

Pregnant female ICR mice (RRID: IMSR_JAX:009122) and 6–8 weeks old male C57BL/6 mice (22–27 g) (RRID: IMSR_JAX:000664) were purchased from Japan SLC (Shizuoka, Japan). All mice were housed in a specific pathogen-free animal facility with a 12 h light/dark cycle (light phase 9:00–21:00) at a density of four mice per cage (17 cm wide × 28 cm long × 13 cm high) under standard conditions (23 ± 1 °C, 50 ± 5% humidity), and food and water were available ad libitum.

Cell Lines

HeLa cells and COS7 cell lines (ATCC, Manassas, VA, USA) were cultured in Dulbecco's modified Eagle's medium (DMEM; Merck, Kenilworth, NJ, USA) containing 10% fetal bovine serum (FBS; Merck), in a humidified atmosphere at 37 °C with 5% CO_2.

Plasmid Constructs

The cDNA encoding human SynGAP1 was purchased from Kazusa DNA Research Institute (Chiba, Japan). The cDNA encoding mouse PSD95 was cloned from mouse cDNA library. The cDNA encoding rat CaMKIIα-full-length and -CA (1–274 aa) were kindly provided by Dr. Watanabe (Showa Pharmaceutical University, Tokyo, Japan). The PCR-amplified cDNA encoding full-length or fragments of SynGAP1, PSD95 or CaMKIIα was subcloned into pCR-Blunt-TOPO vector (Thermo Fisher Scientific, Waltham, MA, USA). After sequencing, these cDNAs were further subcloned into pCAGGS-myc-KK1 [42], pEF-BOS-GST [43] or pEGFP-C1 (Takara Bio Inc, Shiga, Japan) expression vectors. The mutant SynGAP1-S842A was generated with a PrimeSTAR Mutagenesis Basal Kit (Takara) by changing Ser842 to alanine. pGEX-14-3-3ζ was obtained as previously described [14]. pEF-BOS-HA-Rho-kinase-CAT and -RB/PH (TT) were obtained as previously described [44, 45]. GST-fusion proteins were produced in BL21 (DE3) Escherichia coli cell and purified on glutathione-Sepharose 4B beads (GE Healthcare, Chicago, IL, USA).

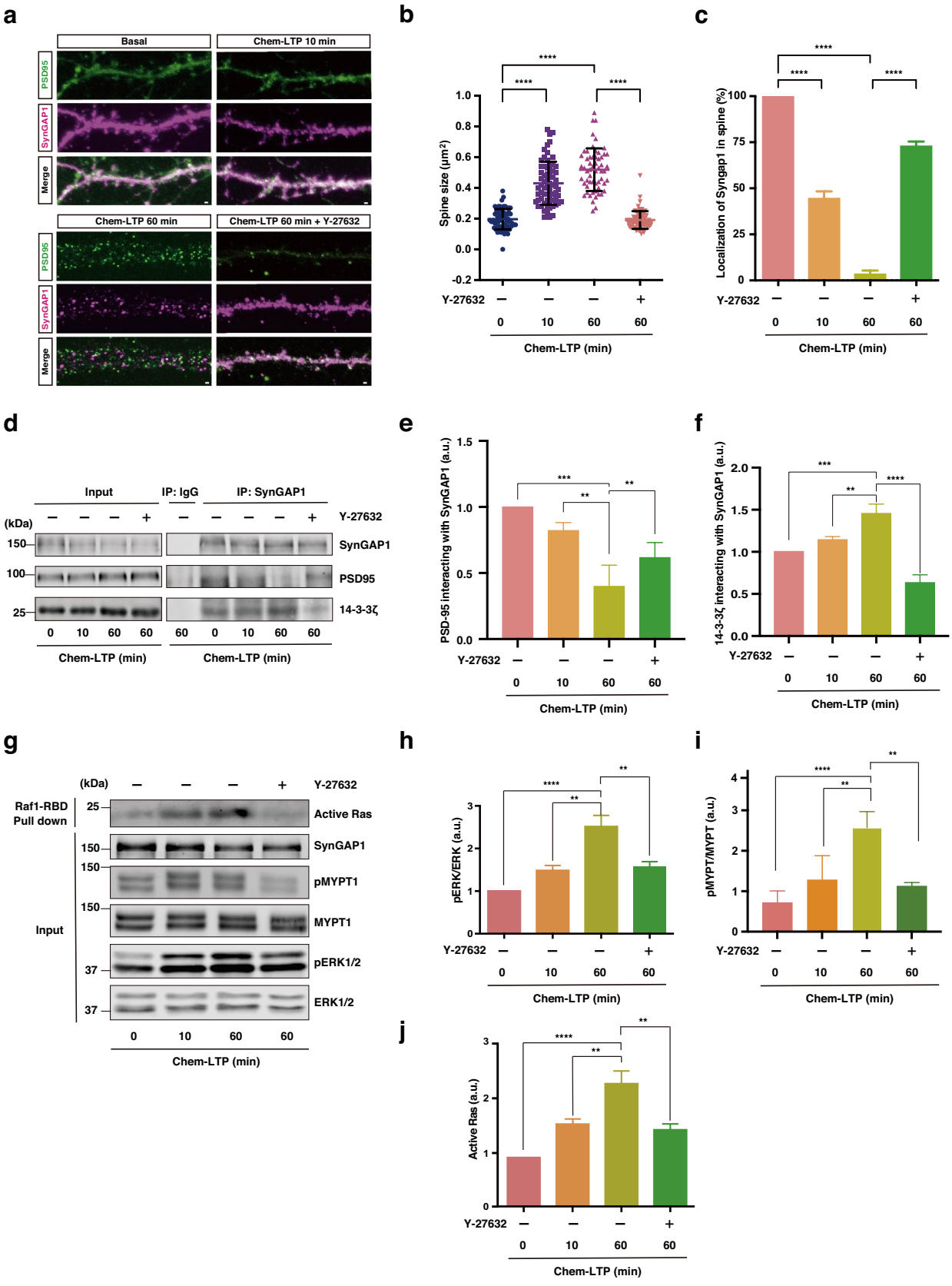
a
Basal
Chem-LTP 10 min
PSD95
SynGAP1
Merge
Chem-LTP 60 min
Chem-LTP 60 min + Y-27632
b
Spine size (μm²)
Y-27632
Chem-LTP (min)
c
Localization of Syngap1 in spine (%)
d
Input
IP: IgG
IP: SynGAP1
(kDa)
SynGAP1
PSD95
14-3-3ζ
e
PSD-95 interacting with SynGAP1 (a.u.)
f
14-3-3ζ interacting with SynGAP1 (a.u.)
g
Raf1-RBD Pull down
Active Ras
Input
pMYPT1
MYPT1
pERK1/2
ERK1/2
h
pERK/ERK (a.u.)
i
pMYPT/MYPT (a.u.)
j
Active Ras (a.u.)

◂**Fig. 5** Phosphorylation of SynGAP1 by Rho-kinase regulates its synaptic localization. **a** Striatal neurons were cultured for 21 days, treated with DMSO or Y-27632 (20 μM) and induced glycine-induced chemical LTP for 10 min or 60 min. Neurons were fixed and immunostained with anti-PSD95 and anti-SynGAP1 antibodies. **b** The dot plot shows the spine size. Data represent the mean ± SEM of three independent experiments and were analyzed by one-way ANOVA with Tukey's post hoc test. ****P < 0.0001. **c** The bar graph shows the amount of localization of SynGAP1 in the spine. Data represent the mean ± SEM of ten independent experiments and were analyzed by one-way ANOVA with Tukey's post hoc test. ****P < 0.0001. **d** Striatal neurons were cultured for 21 days, treated with DMSO or Y-27632 (20 μM) and induced glycine-induced chemical LTP for 10 min or 60 min. Cell lysates were incubated with anti-SynGAP1 antibody for 1 h and then with Protein A Sepharose 4 Fast Flow beads for 1 h. Samples were analyzed by immunoblotting with anti-SynGAP1, anti-PSD95 and anti-14-3-3ζ antibodies. **e** The bar graph shows the amounts of PSD95 interacting with SynGAP1. Data represent the mean ± SEM of three independent experiments and were analyzed by one-way ANOVA with Tukey's post hoc test. **P < 0.01. ***P < 0.001. **f** The bar graph shows the amounts of 14-3-3ζ interacting with SynGAP1. Data represent the mean ± SEM of three independent experiments and were analyzed by one-way ANOVA with Tukey's post hoc test. **P < 0.01. ***P < 0.001. ****P < 0.0001. **g** Striatal neurons were cultured for 21 days, treated with DMSO or Y-27632 (20 μM) and induced glycine-induced chemical LTP for 10 min or 60 min. Cell lysates were incubated with GST-Raf1-RBD to precipitate active Ras, which was followed by immunoblotting with anti-Ras, anti-SynGAP1, anti-pMYPT1 (T853), anti-MYPT1, anti-pERK1/2, and anti-ERK1/2 antibodies. **h** The bar graph shows the relative intensity of pERK1/2 normalized to total ERK1/2. Data represent the mean ± SEM of four independent experiments and were analyzed by one-way ANOVA with Tukey's post hoc test. **P < 0.01. ****P < 0.0001. **i** The bar graph shows the relative intensity of pMYPT1 normalized to total MYPT1. Data represent the mean ± SEM of four independent experiments and were analyzed by one-way ANOVA with Tukey's post hoc test. **P < 0.01. ****P < 0.0001. **j** The bar graph shows amounts of active Ras. Data represent the mean ± SEM of four independent experiments and were analyzed by one-way ANOVA with Tukey's post hoc test. **P < 0.01. ****P < 0.0001

Antibody

Rabbit polyclonal antibody against SynGAP1 phosphorylated at Ser842 (anti-pS842 antibody) was produced against the phosphopeptide C + VNKSVpSMLDLQ (FUJIFILM Wako, Osaka, Japan). We purified an anti-phospho SynGAP1 antibody against the phosphopeptide by an affinity column. In brief, we first prepared an affinity column with phosphopeptide by applying peptide in a Sulfolink coupling gel (Thermo Fisher Scientific), which was followed by blocking the nonspecific binding site by adding cysteine buffer (50 mM L-cysteine HCl, 50 mM Tris–HCl, 5 mM EDTA, pH 8.5). Next, we applied antiserum to the column with overnight rotation at 4 °C. Then, after washing with PBS, we eluted the antibody with 100 mM glycine solution (pH 2.5), and the pH was adjusted to 7.5. Rabbit polyclonal anti-MBS (MYPT1) antibody was generated by use of GST-rat MBS-N-terminal domain (1-707 aa). The following antibodies were obtained commercially: rabbit polyclonal anti-SynGAP1 antibody (RRID:AB_303723) (Abcam, Cambridge, UK), rabbit polyclonal anti-phospho-MYPT1 (T853) antibody (RRID:AB_310812) (Merck), mouse monoclonal anti-PSD95 antibody (RRID:AB_795156) (Thermo Fisher Scientific), rabbit polyclonal anti-c-myc (A-14) (RRID: AB_631274), mouse monoclonal pan-14-3-3 (H-8) (RRID:AB_626618), mouse monoclonal 14-3-3β (A-6) (RRID:AB_626617), mouse monoclonal 14-3-3γ (D-6) (RRID:AB_2818976), mouse monoclonal 14-3-3ε (8C3) (RRID:AB_626619), mouse monoclonal 14-3-3η (6A12) (RRID:n/a), mouse monoclonal 14-3-3σ (E-11) (RRID:AB_2285808), mouse monoclonal 14-3-3θ (5J20) (RRID:AB_2218224), and mouse monoclonal 14-3-3ζ(1B3) (RRID:n/a) antibodies (Santa Cruz, Dallas, TX, USA), mouse anti-GFP antibody (RRID: AB_390913) (Roche, Mannheim, Germany), mouse monoclonal anti-glutathione S-transferase antibody (AB_2883970) (FUJIFILM Wako), rabbit monoclonal anti-SynGAP1 (RRID: AB_11141232), rabbit polyclonal anti-14-3-3 (Pan) (RRID: AB_10860606), rabbit monoclonal anti-Ras (RRID:AB_2269641), rabbit monoclonal anti-PSD95 (RRID: AB_1264242), rabbit monoclonal anti-phospho-p44/42 MAPK (ERK1/2) (T202/Y204) (RRID: AB_2315112), and mouse monoclonal anti-p44/42 MAPK (ERK1/2) (RRID: AB_10695739) antibodies (Cell Signaling Technology Inc, Daners, MA, USA). Following secondary antibodies were also obtain commercially: donkey polyclonal anti-rat IgG with Alexa Fluor 488 (RRID: AB_2535794), donkey polyclonal anti-rabbit IgG with Alexa Fluor 555 (RRID: AB_162543), goat polyclonal anti-rabbit IgG with Alexa Fluor 680 (RRID: AB_2535758), goat polyclonal anti-mouse IgG with Alexa Fluor 680 (RRID: AB_2535724) (Thermo Fisher Scientific) and goat anti-mouse IgG (H + L DyLight 800 Conjugate) (RRID: AB_10693543) (Cell Signaling Technology). The following reagents were used: dimethyl sulfoxide (DMSO) (Merck), Okadaic acid and Y-27632 (FUJIFILM Wako).

Primary Striatal Neuron Cultures and Immunofluorescence Analysis

Cultured neurons were prepared for E15 mouse embryos of ICR female mice (Japan SLC) as described previously [46, 47] with some modifications. Neuron dissociation solutions (FUJIFILM Wako) were used to digest the striatal tissues following the manufacturer's instructions. Dissociated striatal neurons cultured in neurobasal medium (Thermo Fisher Scientific) containing 10% FBS (Merck) were seeded on culture dishes with PDL (poly-D-lysine; Merck) or slides with coverslips. The medium was changed to neurobasal medium containing B-27 supplement (Thermo Fisher Scientific) and 1 mM GlutaMAX (Thermo Fisher Scientific) after 1 h of plating. The neurons were incubated in a

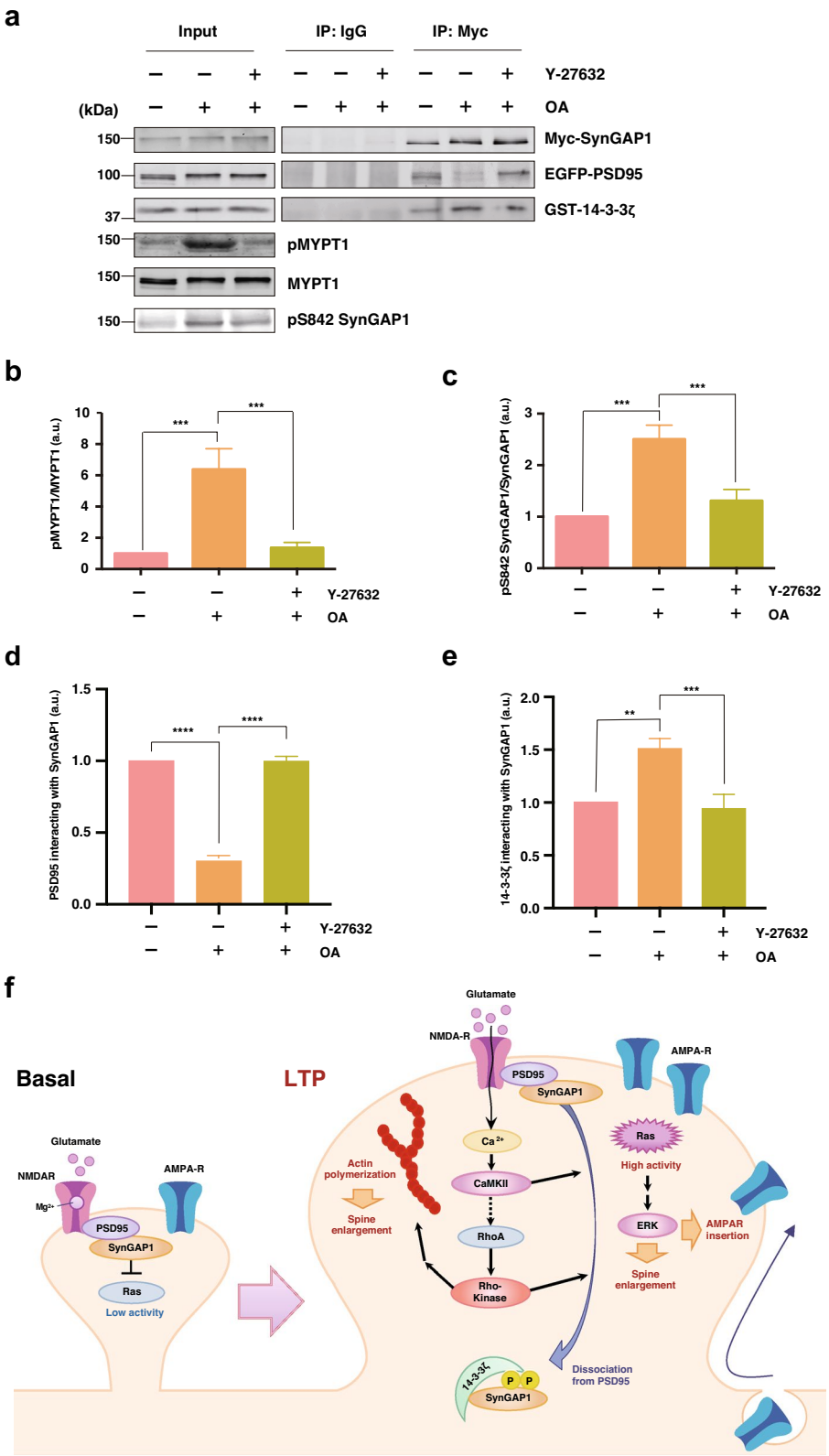

Fig. 6 Rho-kinase decreases the interaction between SynGAP1 and PSD95. **a** Myc-SynGAP1, EGFP-PSD95, and GST-14-3-3ζ were cotransfected into HeLa cells. Cells were treated with DMSO or Y-27632 (20 μM) for 1 h and then stimulated with OA (1 μM) for 1 h. Cell lysates were incubated with anti-Myc antibody, and the immunoprecipitates were analyzed by immunoblotting with anti-Myc, anti-GFP, anti-GST, anti-pSynGAP1 (S842), anti-pMYPT1 (T853), and anti-MYPT1 antibodies. **b** The bar graph shows the relative intensity of pMYPT1 normalized to total MYPT1. Data represent the mean ± SEM of three independent experiments and were analyzed by one-way ANOVA with Tukey's post hoc test. ***$P < 0.001$. **c** The bar graph shows the relative intensity of pSynGAP1 (S842) normalized to total SynGAP1. Data represent the mean ± SEM of three independent experiments and were analyzed by one-way ANOVA with Tukey's post hoc test. ***$P < 0.001$. **d** The bar graph shows the amounts of PSD95 interacting with SynGAP1. Data represent the mean ± SEM of three independent experiments and were analyzed by one-way ANOVA with Tukey's post hoc test. ****$P < 0.0001$. **e** The bar graph shows amounts of 14-3-3ζ interacting with SynGAP1. Data represent the mean ± SEM of three independent experiments and were analyzed by one-way ANOVA with Tukey's post hoc test. **$P < 0.01$. ***$P < 0.001$. **f** The mechanism by which the RhoA-Rho-kinase signal regulates Ras-ERK signaling during LTP induction

humidified atmosphere at 37 °C with 5% CO_2. The cultured striatal neurons were treated with chemically-induced long-term potentiation (Chemical-LTP) and Y-27632 (20 μM). The neurons were fixed with 4% paraformaldehyde in PBS for 20 min at room temperature and permeabilized in PBS containing 0.1% Triton X-100 and 5% normal goat serum for 20 min. The cells were probed with the indicated primary antibodies followed by secondary antibodies conjugated to Alexa Fluor488 and Alexa Fluor555 (Thermo Fisher Scientific). Fluorescence images were acquired with an LSM 780 under the control of LSM software (Carl Zeiss).

Preparation and Incubation of Striatal Slices

Striatal slices were prepared from mice as described previously [17]. Male C57BL/6 mice 6–8 weeks old were decapitated. The brains were rapidly removed and placed in ice-cold, oxygenated Krebs-HCO_3^- buffer (124 mM NaCl, 4 mM KCl, 26 mM $NaHCO_3$ 1.5 mM $CaCl_2$, 1.25 mM MKH_2PO_4, 1.5 mM $MgSO_4$, and 10 mM D-glucose, pH 7.4). Coronal slices (350 μm) were prepared using a VT1200S vibratome (Leica Microsystems, Nussloch, Germany). The stratum was dissected from the slices in ice-cold Krebs-HCO_3^- buffer. Each slice was placed in a polypropylene incubation tube with 2 ml of fresh Krebs-HCO_3^- buffer containing adenosine deaminase (10 μg/ml). The slices were preincubated at 30 °C under constant oxygenation with 95% O_2/5% CO_2 for 60 min. The buffer was replaced with fresh Krebs-HCO_3^- buffer after 30 min of preincubation. The slices were treated with DMSO or Y-27632 for 1 h and then stimulated with okadaic acid for 1 h. After the drug treatments, the slices were transferred to Eppendorf tubes, frozen on dry ice, and stored at − 80 °C until further analysis. Prior to the immunoblot analysis, the slices were mixed by boiling in SDS sample buffer.

Chemical LTP

The Chemical LTP was performed as described previously [26], with some modifications. Cultured dissociated striatal neurons were perfused with warmed/oxidized normal ACSF solution (nACSF: 125 mM NaCl, 2.5 mM KCl, 2 mM $CaCl_2$, 1 mM $MgCl_2$, 5 mM HEPES and 33 mM glucose; pH: 7.3 Osm: 290), then the nACSF solution was discarded, warmed oxidized cLTP solution (cLTP: 125 mM NaCl, 2.5 mM KCl, 2 mM $CaCl_2$, 5 mM Hepes, 33 mM glucose, 0.0005 mM TTX, 0.02 mM bicuculline, and 0.003 mM strychnine) was added for 10 min, and the cells were perfused with glycine (in HBSS: fincal conc. 200 μM) for 5 min. Finally, nACSF was refused again, and the neurons were cultured for 10 min or 60 min.

In vitro Phosphorylation Assay

The in vitro phosphorylation assay was performed as described previously [33, 44]. SynGAP1 fragments were expressed in COS7 cells as GST fusion proteins and purified with glutathione-Sepharose 4B beads (GE Healthcare). The kinase reactions for Rho-kinase were performed in 100 μl of a reaction mixture (50 mM Tris/HCl, pH 7.5, 1 mM EDTA, 1 mM EGTA, 1 mM DTT, 5 mM $MgCl_2$, and 100 μM [γ- ^{32}P] ATP [1–20 GBq/mmol]), with 0.05 μM of the catalytic domain of Rho-kinase and purified GST-SynGAP1 fragments for 20 min at 30 °C. The reaction mixtures were then boiled in sodium dodecyl sulfate (SDS) sample buffer and subjected to SDS-polyacrylamide gel electrophoresis (PAGE) and silver staining. Then, the radiolabeled proteins were visualized with an image analyzer (FLA9000; GE Healthcare).

GST-14-3-3ζ Pulldown Assay

Mouse striatal slices, cultured striatal neurons, or HeLa cells were lysed in lysis buffer [20 mM Tris/HCl, 1 mM EDTA, 150 mM NaCl, 1% NP-40, protease inhibitor cocktail (Roche), and phosphatase inhibitor cocktail (PhosStop, Roche), pH 7.5] and then sonicated 3 times for 5–10 s. After centrifugation at 15,000×*g* for 10 min at 4 °C, the soluble supernatant was incubated with glutathione-Sepharose 4B beads (GE Healthcare) coated with 100 pmol of GST-14-3-3ζ for 1 h at 4 °C with gentle rotation. The beads were washed three times with lysis buffer, eluted by boiling in SDS sample buffer for SDS-PAGE and then subjected to immunoblot analysis with the indicated antibodies.

Active Ras Pulldown Assay (GST-Raf1-RBD Pulldown Assay)

Myc-SynGAP1-WT or Myc-SynGAP1-S842A was cotransfected with HA-Rho-kinase CAT or HA-Rho-kinase-RB/PH (TT) into HeLa cells. After 18–24 h of transfection, HeLa cells were lysed in lysis buffer [20 mM Tris/HCl, 1 mM EDTA, 150 mM NaCl, 1% NP-40, protease inhibitor cocktail (Roche), and phosphatase inhibitor cocktail (PhosStop, Roche), pH 7.5] and then sonicated 3 times for 5 s. The cell lysate, which was obtained by centrifugation at 15,000×*g* for 10 min at 4 °C, was then incubated with glutathione-Sepharose 4B beads (GE Healthcare) coated with 100 pmol of GST-Raf1-RBD for 1 h at 4 °C with gentle rotation. Active Ras was pulled down by beads attached to Raf1-RBD. The beads were washed three times with lysis buffer, eluted by boiling in SDS sample buffer for SDS-PAGE and

then subjected to immunoblot analysis with the indicated antibodies.

Immunoprecipitation Assay

Mouse brains, cultured striatal neurons, or HeLa cells were lysed in lysis buffer [20 mM Tris/HCl, 1 mM EDTA, 150 mM NaCl, 1% NP-40, protease inhibitor cocktail (Roche), and phosphatase inhibitor cocktail (PhosStop, Roche), pH 7.5] and then sonicated 3 times for 5–10 s. The lysate was incubated for 30 min at 4 °C with rotation and centrifuged at 15,000×*g* for 10 min at 4 °C. The supernatant was used as the cell lysate. The indicated antibodies were incubated with the lysate for 1 h with rotation and then with Protein A Sepharose 4 Fast Flow beads (GE Healthcare) for 1 h at 4 °C with gentle rotation. The beads were washed three times with lysis buffer, eluted by boiling in SDS sample buffer for SDS-PAGE and then subjected to immunoblot analysis with the indicated antibodies.

SDS-PAGE and Immunoblot Analysis

Laemmli's SDS-PAGE was carried out using 6%, 8%, or 12% polyacrylamide gels (Nacalai Tesque, Kyoto, Japan). The proteins were separated via SDS-PAGE and transferred to polyvinylidene difluoride membranes (Immobilon- FL, Merck). The membranes were blocked for 30 min at room temperature with Blocking-One (Nacalai Tesque) or Blocking-One P (Nacalai Tesque) and incubated for 1 h at room temperature or overnight at 4 ℃ with primary antibodies. The membranes were washed with 0.05% Tween/TBS and were then incubated with secondary antibodies for 30 min at room temperature. Specific binding was detected using an infrared (LI-COR Biosciences, Lincoln, NE) imaging system. Band intensities were quantified using ImageStudio software (RRID: SCR_015795, LI-COR Biosciences).

Statistical Analysis

Data analysis was performed using Prism 8 Statistics software (RRID: SCR_002798, GraphPad Software, Inc., La Jolla, USA). All data are expressed as the mean ± standard error of the mean (SEM). One-way or two-way analysis of variance (ANOVA) was used followed by Tukey's multiple-comparison test when the F ratios were significant ($p < 0.05$). Student's t test was used to compare the difference between two groups. No blinding was performed, and $p < 0.05$ was considered to indicate statistical significance.

Supplementary Information The online version contains supplementary material available at https://doi.org/10.1007/s11064-022-03623-y.

Acknowledgements We are grateful to T. Watanabe, T. Nishioka, K. Kuroda, S. Kozawa and other Kaibuchi laboratory members for helpful discussions and preparation of some materials, T. Ishii for secretarial assistance, and S. Furuta for life support. We also thank the Division for Research on Laboratory Animals, the Radioisotope Center Medical Branch and Medical Research Engineering of Nagoya University Graduate School of Medicine and the Education and Research Center of Animal Models for Human Diseases in Fujita Health University.

Author Contributions Conceptualization: [MW, YF, TT, KK]; Methodology: [MW, YF, DT, MA]; Formal analysis and investigation: [MW, YF, EH, RUA, MA]; Writing—original draft preparation: [MW]; Writing—review and editing: [YF, KK]; Funding acquisition: [MW, YF, DT, MA, KK]; Resources: [YF, TT, DT, MA]; Supervision: [KY, KK]. All authors provided critical feedback and helped shape the research, analysis, and manuscript. All authors approved the final version submitted.

Funding This work was supported by the following funding sources: ''Bioinformatics for Brain Sciences'' performed under the SRPBS from MEXT and AMED (KK); AMED Grant Nos. JP21dm0207075 (KK), JP21wm0425017 (YF); JSPS KAKENHI Grant Nos. JP17H01380 (KK), JP17J09461 (MW), JP17K07383 (MA), JP18K14849 (YF), JP21K06428 (YF), JP21K06427 (DT); MEXT KAKENHI Grant Nos. JP19H05209 (KK), JP21H00196 (KK); the Uehara Science Foundation (KK, YF), the Takeda Science Foundation (KK, YF), and the Hori Sciences & Arts Foundation (KK, YF).

Data Availability The datasets generated during this study are available from the corresponding author on reasonable request.

Declarations

Conflict of interest The authors have no relevant financial or non-financial interest to disclose.

Ethical Approval All animal experiments were approved and performed in accordance with the guidelines for the care and use of laboratory animals established by the Animal Experiments Committee of Nagoya University Graduate School of Medicine (Approval Number: 20094) and Fujita Health University (Approval Number: AP20037). All experiments were conducted in compliance with the ARRIVE guidelines.

Consent to Participate Not applicable.

References

1. Anggono V, Huganir RL (2012) Regulation of AMPA receptor trafficking and synaptic plasticity. Curr Opin Neurobiol 22:461–469
2. Kessels HW, Malinow R (2009) Synaptic AMPA receptor plasticity and behavior. Neuron 61:340–350
3. Shepherd JD, Huganir RL (2007) The cell biology of synaptic plasticity: AMPA receptor trafficking. Annu Rev Cell Dev Biol 23:613–643
4. Vitureira N, Goda Y (2013) Cell biology in neuroscience: the interplay between Hebbian and homeostatic synaptic plasticity. J Cell Biol 203:175–186
5. Zeng M, Shang Y, Araki Y, Guo T, Huganir RL, Zhang M (2016) Phase transition in postsynaptic densities underlies formation of synaptic complexes and synaptic plasticity. Cell 166:1163-1175 e1112

6. Lee HK, Barbarosie M, Kameyama K, Bear MF, Huganir RL (2000) Regulation of distinct AMPA receptor phosphorylation sites during bidirectional synaptic plasticity. Nature 405:955–959
7. Krapivinsky G, Medina I, Krapivinsky L, Gapon S, Clapham DE (2004) SynGAP-MUPP1-CaMKII synaptic complexes regulate p38 MAP kinase activity and NMDA receptor-dependent synaptic AMPA receptor potentiation. Neuron 43:563–574
8. Murakoshi H, Yasuda R (2012) Postsynaptic signaling during plasticity of dendritic spines. Trends Neurosci 35:135–143
9. Murakoshi H, Wang H, Yasuda R (2011) Local, persistent activation of Rho GTPases during plasticity of single dendritic spines. Nature 472:100–104
10. Kasai H, Ziv NE, Okazaki H, Yagishita S, Toyoizumi T (2021) Spine dynamics in the brain, mental disorders and artificial neural networks. Nat Rev Neurosci 22:407–422
11. Lisman J, Yasuda R, Raghavachari S (2012) Mechanisms of CaMKII action in long-term potentiation. Nat Rev Neurosci 13:169–182
12. Thomas GM, Huganir RL (2004) MAPK cascade signalling and synaptic plasticity. Nat Rev Neurosci 5:173–183
13. Nishioka T, Amano M, Funahashi Y, Tsuboi D, Yamahashi Y, Kaibuchi K (2019) In vivo identification of protein kinase substrates by kinase-oriented substrate screening (KIOSS). Curr Protoc Chem Biol 11:e60
14. Nishioka T, Nakayama M, Amano M, Kaibuchi K (2012) Proteomic screening for Rho-kinase substrates by combining kinase and phosphatase inhibitors with 14-3-3zeta affinity chromatography. Cell Struct Funct 37:39–48
15. Muslin AJ, Tanner JW, Allen PM, Shaw AS (1996) Interaction of 14-3-3 with signaling proteins is mediated by the recognition of phosphoserine. Cell 84:889–897
16. Nishioka T, Nakayama M, Amano M, Kaibuchi K (2012) Proteomic screening for Rho-kinase substrates by combining kinase and phosphatase inhibitors with 14-3-3ζ affinity chromatography. Cell Struct Funct 7:39–48
17. Nagai T, Nakamuta S, Kuroda K, Nakauchi S, Nishioka T, Takano T, Zhang X, Tsuboi D, Funahashi Y, Nakano T, Yoshimoto J, Kobayashi K, Uchigashima M, Watanabe M, Miura M, Nishi A, Kobayashi K, Yamada K, Amano M, Kaibuchi K (2016) Phosphoproteomics of the dopamine pathway enables discovery of Rap1 activation as a reward signal in vivo. Neuron 89:550–565
18. Nagai T, Yoshimoto J, Kannon T, Kuroda K, Kaibuchi K (2016) Phosphorylation signals in striatal medium spiny neurons. Trends Pharmacol Sci 37:858–871
19. Ahammad RU, Nishioka T, Yoshimoto J, Kannon T, Amano M, Funahashi Y, Tsuboi D, Faruk MO, Yamahashi Y, Yamada K, Nagai T, Kaibuchi K (2021) Kanphos: a database of kinase-associated neural protein phosphorylation in the brain. Cells 11(1):47
20. Chen HJ, Rojas-Soto M, Oguni A, Kennedy MB (1998) A synaptic Ras-GTPase activating protein (p135 SynGAP) inhibited by CaM kinase II. Neuron 20:895–904
21. Kim JH, Liao D, Lau LF, Huganir RL (1998) SynGAP: a synaptic RasGAP that associates with the PSD-95/SAP90 protein family. Neuron 20:683–691
22. Bos JL, Rehmann H, Wittinghofer A (2007) GEFs and GAPs: critical elements in the control of small G proteins. Cell 129:865–877
23. Jeyabalan N, Clement JP (2016) SYNGAP1: Mind the Gap. Front Cell Neurosci 10:32
24. Llamosas N, Arora V, Vij R, Kilinc M, Bijoch L, Rojas C, Reich A, Sridharan B, Willems E, Piper DR, Scampavia L, Spicer TP, Miller CA, Holder JL, Rumbaugh G (2020) SYNGAP1 controls the maturation of dendrites, synaptic function, and network activity in developing human neurons. J Neurosci 40:7980–7994
25. Noboru H, Komiyama AMW, Carlisle Holly J, Porter Karen, Charlesworth Paul, Jennifer Monti DJCS, O'Carroll Colin M, Martin Stephen J, Morris Richard G. M, O'Dell Thomas J, Grant Seth G. N (2002) SynGAP regulates ERK:MAPK signaling, synaptic plasticity, and learning in the complex with postsynaptic density 95 and NMDA receptor. J Neurosci 22(22):9721–9732
26. Araki Y, Zeng M, Zhang M, Huganir RL (2015) Rapid dispersion of SynGAP from synaptic spines triggers AMPA receptor insertion and spine enlargement during LTP. Neuron 85:173–189
27. Ikeda M, Hikita T, Taya S, Uraguchi-Asaki J, Toyo-oka K, Wynshaw-Boris A, Ujike H, Inada T, Takao K, Miyakawa T, Ozaki N, Kaibuchi K, Iwata N (2008) Identification of YWHAE, a gene encoding 14-3-3epsilon, as a possible susceptibility gene for schizophrenia. Hum Mol Genet 17:3212–3222
28. Navarrete M, Zhou Y (2022) The 14-3-3 protein family and Schizophrenia. Front Mol Neurosci 15:857495
29. Cornell B, Toyo-Oka K (2017) 14-3-3 proteins in brain development: neurogenesis, neuronal migration and neuromorphogenesis. Front Mol Neurosci 10:318
30. Cheah PS, Ramshaw HS, Thomas PQ, Toyo-Oka K, Xu X, Martin S, Coyle P, Guthridge MA, Stomski F, van den Buuse M, Wynshaw-Boris A, Lopez AF, Schwarz QP (2012) Neurodevelopmental and neuropsychiatric behaviour defects arise from 14-3-3zeta deficiency. Mol Psychiatry 17:451–466
31. Xu X, Jaehne EJ, Greenberg Z, McCarthy P, Saleh E, Parish CL, Camera D, Heng J, Haas M, Baune BT, Ratnayake U, van den Buuse M, Lopez AF, Ramshaw HS, Schwarz Q (2015) 14-3-3zeta deficient mice in the BALB/c background display behavioural and anatomical defects associated with neurodevelopmental disorders. Sci Rep 5:12434
32. Angrand PO, Segura I, Volkel P, Ghidelli S, Terry R, Brajenovic M, Vintersten K, Klein R, Superti-Furga G, Drewes G, Kuster B, Bouwmeester T, Acker-Palmer A (2006) Transgenic mouse proteomics identifies new 14-3-3-associated proteins involved in cytoskeletal rearrangements and cell signaling. Mol Cell Proteomics 5:2211–2227
33. Amano M, Tsumura Y, Taki K, Harada H, Mori K, Nishioka T, Kato K, Suzuki T, Nishioka Y, Iwamatsu A, Kaibuchi K (2010) A proteomic approach for comprehensively screening substrates of protein kinases such as Rho-kinase. PLoS One 5:e8704
34. Medina AE, Liao DS, Mower AF, Ramoa AS (2001) Do NMDA receptor kinetics regulate the end of critical periods of plasticity. Cell Press 32:553–556
35. Hui-Chen Lu, Gonzalez Ernesto, Crair MC (2001) Barrel cortex critical period plasticity is independent of changes in NMDA receptor subunit composition. Cell Press 32:619–634
36. Molnar E (2011) Long-term potentiation in cultured hippocampal neurons. Semin Cell Dev Biol 22:506–513
37. Paul A, Nawalpuri B, Shah D, Sateesh S, Muddashetty RS, Clement JP (2019) Differential regulation of syngap1 translation by FMRP modulates eEF2 mediated response on NMDAR activity. Front Mol Neurosci 12:97
38. Feng W, Zhang M (2009) Organization and dynamics of PDZ-domain-related supramodules in the postsynaptic density. Nat Rev Neurosci 10:87–99
39. Kim E, Sheng M (2004) PDZ domain proteins of synapses. Nat Rev Neurosci 5:771–781
40. Walkup WG, Washburn L, Sweredoski MJ, Carlisle HJ, Graham RL, Hess S, Kennedy MB (2015) Phosphorylation of synaptic GTPase-activating protein (synGAP) by Ca2+/calmodulin-dependent protein kinase II (CaMKII) and cyclin-dependent kinase 5 (CDK5) alters the ratio of its GAP activity toward Ras and Rap GTPases. J Biol Chem 290:4908–4927
41. Lee KJ, Lee Y, Rozeboom A, Lee JY, Udagawa N, Hoe HS, Pak DT (2011) Requirement for Plk2 in orchestrated ras and rap signaling, homeostatic structural plasticity, and memory. Neuron 69:957–973
42. Nishimura T, Yamaguchi T, Kato K, Yoshizawa M, Nabeshima Y, Ohno S, Hoshino M, Kaibuchi K (2005) PAR-6-PAR-3 mediates

Cdc42-induced Rac activation through the Rac GEFs STEF/Tiam1. Nat Cell Biol 7:270–277
43. Mizushima S, Nagata S (1990) pEF-BOS, a powerful mammalian expression vector. Nucleic Acids Res 18:5322
44. Amano M, Hamaguchi T, Shohag MH, Kozawa K, Kato K, Zhang X, Yura Y, Matsuura Y, Kataoka C, Nishioka T, Kaibuchi K (2015) Kinase-interacting substrate screening is a novel method to identify kinase substrates. J Cell Biol 209:895–912
45. Amano M, Chihara K, Nakamura N, Fukata Y, Yano T, Shibata M, Ikebe M, Kaibuchi K (1998) Myosin II activation promotes neurite retraction during the action of Rho and Rho-kinase. Genes Cells 3:177–188
46. Funahashi Y, Ariza A, Emi R, Xu Y, Shan W, Suzuki K, Kozawa S, Ahammad RU, Wu M, Takano T, Yura Y, Kuroda K, Nagai T, Amano M, Yamada K, Kaibuchi K (2019) Phosphorylation of Npas4 by MAPK regulates reward-related gene expression and Behaviors. Cell Rep 29:3235-3252 e3239
47. Takano T, Wu M, Nakamuta S, Naoki H, Ishizawa N, Namba T, Watanabe T, Xu C, Hamaguchi T, Yura Y, Amano M, Hahn KM, Kaibuchi K (2017) Discovery of long-range inhibitory signaling to ensure single axon formation. Nat Commun 8:33